Proceedings of the ASME Turbo Expo 2017
GT2017
June 26-30, 2017, Charlotte, NC, USA

GT2017-63633

CHARACTERIZATION OF THE MODAL CHARACTERISTICS OF STRUCTURES OPERATING IN DENSE LIQUID TURBOPUMPS

Joseph Chiu
City College of New York
New York, New York

Andrew M. Brown
NASA/Marshall Space Flight Center
Huntsville, Al 35812

ABSTRACT

It is well-known that the natural frequencies of structures immersed in heavy liquids will decrease due to the fluid "added-mass" effect. This reduction has not been precisely determined, though, with indications that it is in the 20-40% range for water. In contrast, the mode shapes of these structures have always been assumed to be invariant in liquids. Recent modal testing at NASA/Marshall Space Flight Center of turbomachinery inducer blades in liquid oxygen, which has a density slightly greater than water, indicates that the mode shapes change appreciably, though. This paper presents a study that examines and quantifies the change in mode shapes as well as more accurately defines the natural frequency reduction. A literature survey was initially conducted and test-verified analytical solutions for the natural frequency reductions were found for simple geometries, including a rectangular plate and an annular disk. The ANSYS© fluid/structure coupling methodology was then applied to obtain numerical solutions, which compared favorably with the published results. This initial study indicated that mode shape changes only occur for non-symmetric boundary conditions. Techniques learned from this analysis were then applied to the more complex inducer model. ANSYS numerical results for both natural frequency and mode shape compared well with modal test in air and water. A number of parametric studies were also performed to examine the effect of fluid density on the structural modes, reflecting the differing propellants used in rocket engine turbomachinery. Some important findings were that the numerical order of mode shapes changes with density initially, and then with higher densities the mode shapes themselves warp as well. Valuable results from this study include observations on the causes and types of mode shape alteration and an improved prediction for natural frequency reduction in the range of 30-41% for preliminary design. Increased understanding and accurate prediction of these modal characteristics is critical for assessing resonant response, correlating finite element models to modal test, and performing forced response in turbomachinery.

NOMENCLATURE

IP	In Phase
OP	Out of Phase
MAC	Modal Assurance Criterion
MN	Mode Number
MS	Mode Shape
LH2	Liquid Hydrogen
LOX	Liquid Oxygen

INTRODUCTION

During the design of the J2-X rocket engine in 2012, preliminary analysis of the two inducer blades in the Liquid Oxygen (LOX) turbopump (Figure 1) predicted high stresses from a possibly resonant dynamic forcing function. It is well-known that the natural frequencies of a structure decrease when it is immersed in a fluid due to the effective added-mass, so a "knockdown factor", which is the percentage that the natural frequencies decrease, was applied to the frequencies in the Campbell Diagram, but previously-used factors based on anecdotal experience was tremendously inconsistent, with a range of between 20 and 40%. A modal test was therefore performed to find the natural frequencies of the J2-X inducer blades immersed in water, which has a density slightly greater than LOX, to enable accurate prediction of resonance and for the model verification critical for forced response analysis.

The blades were tested in both air and water, and in several different housing configurations to examine the effects of tip clearance and grooves in the housing. The results indicated that in addition to the natural frequency change in water, which was expected, the modes shapes changed as well. There was no indication in initial literature surveys or previous experiments that this would occur, so the result was surprising. These changes made both correlation with the finite element model and use of the model for forced response analysis problematic. An attempt at implementation of a new acoustic/structure finite

element formulation was made, but there were some limitations in the software at that time preventing complete reliance on that technique.

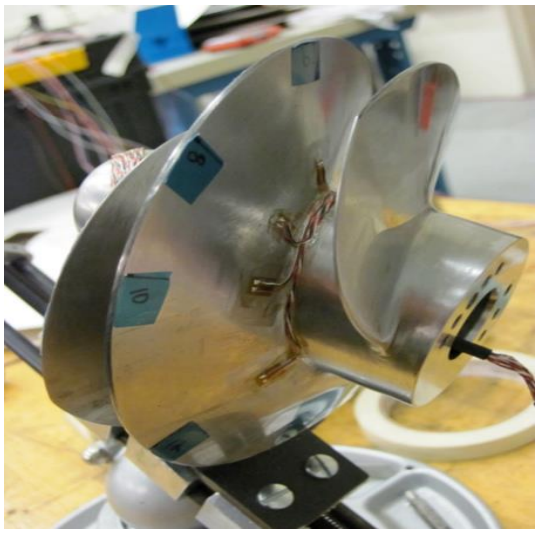

Figure 1. J2-X LOX Turbopump Inducer (not to scale)

There has been some research in this field, but the only research found provides analytical and numerical data on the "knockdown factor", without any mention of mode shape alteration. One of the first studies was by Lindholm [1] in 1965, which presented experimental results for the natural frequencies of a cantilever plate in fluid. No mention is made of a change in the mode shapes, though. Kwak [2] presents an excellent study with both theoretical and experimental results of an annual disk, and Askari [3] develops a more extensive theoretical basis for the frequency reduction for the same geometry. Kerboua [4] develops exact analytical expressions for the fluid added-mass for a flat plate in order to develop the frequency knockdown using some advanced thin-shell theories, but again does not identify the loss of mode shape consistency. Hosseini-Hashimi [5] state that the "simplifying hypothesis that the wet and dry mode shapes are the same, is not assumed in this paper" in their study of Mindlin plates in a fluid, but do not present any investigation into or results for the mode shape change.

This change in the mode shapes has motivated the current study discussed in this paper. The focus is on quantifying the change in mode shapes, developing a methodology to accurately predict the changes, and to attempt to learn why the changes take place. In addition, a more refined quantification of the natural frequency change is sought. In particular, the effect of density on the structural modes of the inducer blades is evaluated for its effect on the modal characteristics.

METHODOLOGY

The general purpose multi-physics/finite element code ANSYS WorkBench 17.0 with the ACT fluid/structure coupling extension is the primary numerical tool used in this study to obtain the modal characteristics of structures immersed in fluids. To gain an understanding of the fluid/structure coupling methodology, simpler geometries are first used to verify that the ANSYS settings accurately represent the physics and that the modal characteristics match results obtained from analytical solutions found in the literature. These geometries include a flat rectangular plate and an annular disk, and are discussed in more detail in the next section. Afterwards, a parametric study is performed for the annular disk to identify the effect of fluid density on its modal characteristics.

After these analyses are completed, the same numerical techniques and settings can be applied to analyze the inducer blades. However, since there is no analytical solution, modal test results are used as a comparison to see if the natural frequencies from the numerical model are in good agreement with these test frequencies. If there is a good match on the modal characteristics, the same parametric study done for the annular disk can now be performed for the inducer blades. Observations and conclusions can then be drawn about how fluid density affects the natural frequencies and mode shapes of the inducer blades. It is important to note that the analyses were performed at room temperature, so the temperature effects on the modal characteristics of the structures are not taken into account. These effects are ignored to isolate the effect of the fluid-added mass on the mode shapes.

FLAT PLATE

The first of the simple geometries examined is a flat rectangular plate with one fixed end. The analytical solutions for the natural frequencies of this configuration in vacuum are shown in equation (1) below, from Blevins [6]

$$f_{ij} = \frac{{\lambda_{ij}}^2}{2\pi a^2}\left[\frac{Eh^3}{12\gamma(1-\nu^2)}\right]^{\frac{1}{2}}; i = 1,2,3\ldots; j = 1,2,3\ldots \quad (1)$$

where a and h are the length and thickness of the plate, respectively, i and j are the numbers of half-waves in the mode shape along its longitudinal and transverse axes, respectively, E is the modulus of elasticity, ν is Poisson's ratio, γ is the mass per unit area, and λ_{ij} as a function of a, b, i, and j is a constant found in Table 11-4 of the Blevin's text. If the structure is immersed in fluid, the frequencies are adjusted using equation (2), also from Blevins

$$\frac{f_{i_{in\ fluid}}}{f_{i_{vacuum}}} = \frac{1}{\left(1+\frac{2A_p}{M_p}\right)^{\frac{1}{2}}} \quad (2)$$

where M_p is the mass of the plate, and A_p is the "added mass", which is a quantification of the fluid that moves with the blade during its modal deformation. The added mass is a function of the fluid and mode shape and is tabulated in Table 14-4 of the Blevins text.

The next step in the process is a numerical analysis. A solid geometry model is initially created with a geometric modeling software such as ANSYS DesignModeler© or SpaceClaim©. A fluid domain is also created using the "enclosure" feature in SpaceClaim©. A transparent view of the model is shown in Figure 2.

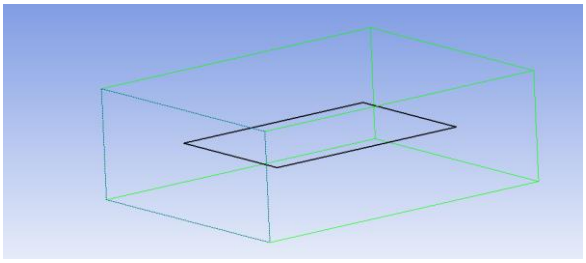

Figure 2. Transparent View of Cantilever Plate Inside Fluid Domain

The model is then imported into ANSYS Mechanical and a modal analysis is performed. The properties of the plate and the fluid domain are listed in Table 1.

Table 1. Properties for Rectangular Plate Analysis

Plate	Fluid Domain
Length=46.736 cm (18 in)	Length =68.58cm (27 in)
Width=30.48 cm (12 in)	Width =53.34 cm (21 in)
Thickness = 0.127 cm (0.05 in)	Height =23.0 cm (9.05in)
Density: 8193 kg/m^3 (7.67e-4 slinch/in^3)	Density =1.06e-5 kg/m^3 (9.36 x 10^{-5} slinch/in^3)
E (Young's Modulus) = 206.84 GPa (3e7 psi)	c (Speed of sound)=148e3 cm/s (58346.46 in/s)
ν (Poisson's Ratio) = 0.27	

ANSYS [7] advises using a fluid domain that is at least half the size wavelength of the fluid as determined in equation (3)

$$\lambda = \frac{c}{f} \tag{3}$$

where λ is the wavelength of the fluid, c is the speed of sound, and f is the highest natural frequency of interest. Setting this size is important, as the modes of the coupled acoustic/structural system are highly dependent upon it, and the goal is to avoid acoustic modes if structure-only modes are being sought. However, too large of a domain will make the solution computationally intensive, so some iteration is required to establish convergence without too much expense. Convergence in this case was reached with the dimensions as shown, which are only about half of the recommended size for water.

If it is known a-priori that coupled acoustic-structure modes are not of interest, then the speed of sound can be set to a very high value, or equivalently, an "incompressible" flag in the software can be set to move the acoustic modes well out of the range of the structural modes while maintaining the mass-added effect of the fluid. Of course, this uncoupled assumption must be carefully made, as studies have shown significant and unanticipated effects of structural-acoustic coupling in turbomachinery, particularly in LH2 [8].

The next step is to perform the pre-processing for the finite element model of the fluid and structure. A high-density tetrahedral mesh option is used for the fluid elements, and three-element thick hexagonal elements are used for the plate. For the fluid and the structural domains to be coupled successfully, the nodes of the plate must be coincident with nodes of the fluid, as shown in Figure 3. The acoustic body condition is then specified for the fluid domain, enabling the application of fluid elements, and the fluid/structure interface is identified at all the faces of the plate.

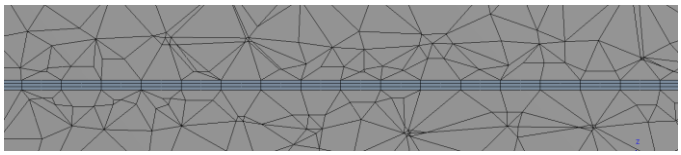

Figure 3. Coincident Nodes at Fluid/Structure Interface

At this point the modal characteristics of the cantilever plate can be obtained. Two analyses are performed to compare the natural frequencies and mode shapes in vacuum and then in water. We use Blevin's categorization scheme in which each mode shape is identified by the number of half waves along the length followed by the number of half waves along the width, e.g., mode 1,3 has one length-wise half wave and three width-wise half waves. To enable a consistent relationship between the modal characteristics and fluid density independent of the use of the acoustic fluid/structure formulation, the vacuum case was always performed using fluid elements with a negligible density. The natural frequencies found using the analytical solution are in good agreement with the natural frequencies found using the numerical model for this vacuum case; five of the first six natural frequencies have relative error percentages less than 1% and the sixth is under 1.5%. On the other hand, most of the natural frequency values for water had relative errors between the numerical and analytical results of well over 10%, as shown in Table 2.

Table 2. Nat. Frequency Comparison, Water

Mode Shape	**1,1**	**1,2**	**2,1**	**2,2**	**1,3**	**3,1**
analytical nat. freq's (h**z**)	1.03	5.48	6.43	18.54	27.09	18.43
FEA nat. freq's (h**z**)	1.24	5.85	8.82	20.86	31.74	28.28
relative error (%)	20.5	6.7	37.3	12.6	17.1	53.4

Upon close examination, it appears that the mode shapes themselves change when submerged in water, as shown by

modes 5 and 6 in Figure 4. These changes probably explain the frequency discrepancy to some degree.

Even though the modal categorization stays the same, it can be clearly seen that the character of the mode has changed. It is therefore necessary to use the more quantitative measure of the change in character of the modes shapes expressed by the Modal Assurance Criteria, which is obtained automatically using an extension in ANSYS.

$$MAC = \frac{\{\varphi_T\}^T\{\varphi_A\}}{(\{\varphi_T\}^T\{\varphi_T\})(\{\varphi_A\}^T\{\varphi_A\})} \quad (4)$$

The MAC describes the degree of consistency (linearity) between one mode and another reference mode, with a value of one indicating perfect agreement.

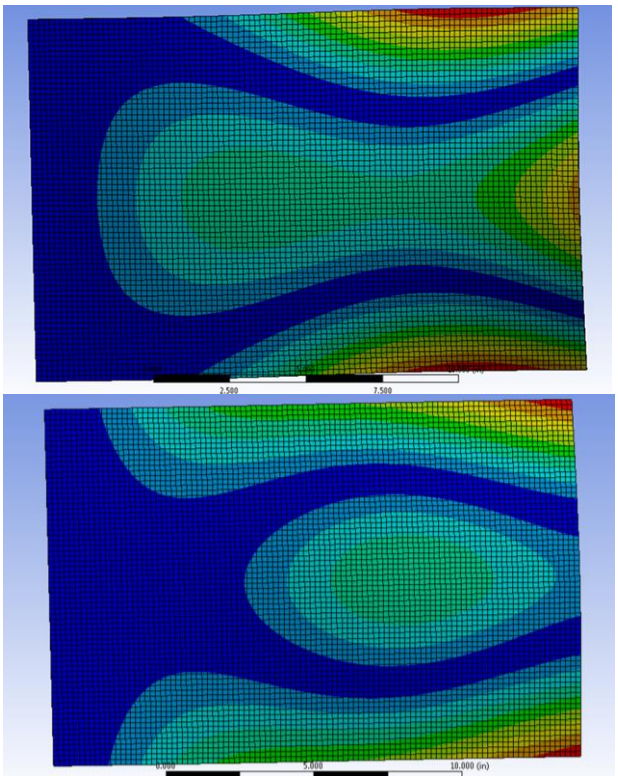

Figure 4. VA Mode Number 6 (Mode Shape 1,3) on top, Water Mode Number 5 (Mode Shape 1,3) on bottom

Table 3. MAC Values for Cantilever Plate

		Mode Shapes for Vacuum					
Mode Shapes for Water		**1**	**2**	**3**	**4**	**5**	**6**
	1	1	0	0	0	0	0
	2	0	1	0	0	0	0
	3	0.116	0	0.882	0	0.001	0.001
	4	0	0.022	0	0.976	0	0
	5	0.003	0	0.106	0	0.407	0.471
	6	0.063	0	0.001	0	0.623	0.311

Comparisons between the first six modes in water and vacuum are shown in Table 3, where values larger than 0.9 are highlighted. The qualitative observation concerning the differences in vacuum mode 6 and water mode 5 previously mentioned is supported by the MAC calculation of only 0.471.

It appears that the mode number (or order) mismatch and mode shape change may have caused the error between the analytical and numerical natural frequencies. Blevins does not mention mode shapes changing in equation (2), though the mode number mismatch may be explained through the fact that different plate added masses are used for different mode shapes in his theoretical formula; the increase in fluid density may lead to mode number mismatch, as the natural frequency for one particular mode shape may change faster than for another mode shape. As the fluid density becomes larger, this change in added mass may become significant enough for a mode number to switch with another mode number, which is the case for the cantilever plate.

Fixed-Fixed Plate

To examine the effect of boundary conditions on the change in mode shapes, a fixed support is applied to both short ends of the plate and an analysis performed. The resulting analytical/numerical frequency errors are much lower, being under 1% for all vacuum modes and only one case over 11% for the water modes.

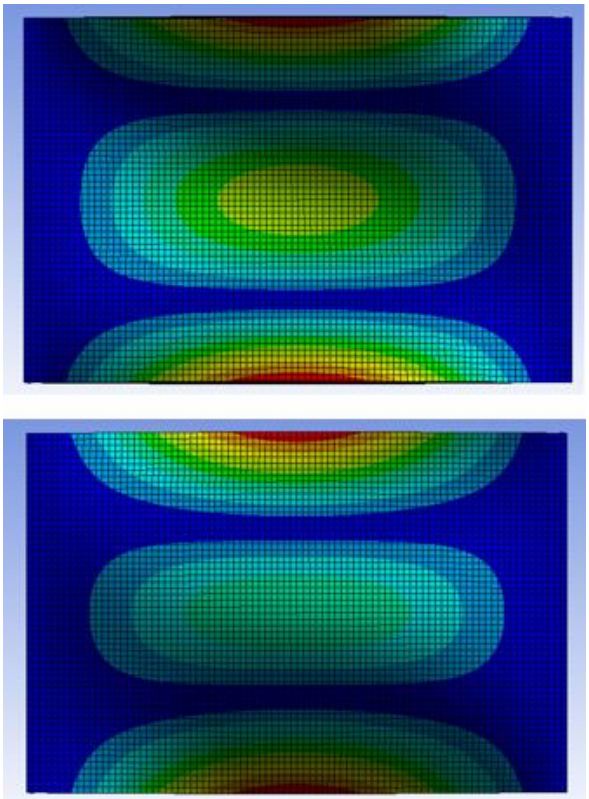

Figure 5. Vacuum Mode Number 4 (Mode Shape 1,3) on top, Water Mode Number 5 (Mode Shape 1,3) on bottom

The modal results show mainly mode number mismatches, with no changes in the essential modes shapes, although there is a small change in the relative magnitudes of the mode shapes, as shown in Figure 5. This can be attributed to the different rates that the added mass increases by depending on the mode shape, which is the same case for the cantilever plate.

MAC results also clearly show this result, with qualitatively well-matching mode pairs yielding values very close to one, but these numbers not always being on the diagonal, indicating the modal number mismatch. Comparing these results with those from the cantilever plate, it appears that symmetry plays a role in whether the mode shapes change or not, as the mode shapes change for a non-symmetric cantilever plate but do not for the symmetric fixed-fixed plate.

ANNULAR DISK

An examination is now performed based upon the work by Kwak described previously. He develops the following equation for this geometry submerged in a liquid:

$$f_w = \frac{f_a}{\sqrt{1+\Gamma\beta}} \quad , \quad \beta = \frac{\rho_w a}{\rho_p h} \qquad (5)$$

where f_w is the natural frequency in water, f_a is the natural frequency in air, Γ is the Nondimensionalized Added Virtual Mass Incremental (NAVMI) factor, β is the thickness correction factor, ρ_w is the density of water, ρ_p is the mass density of the disk, a is the outer radius of the disk, and h is the thickness of the disk. An experiment is also presented in the paper for a steel disk of 200 mm outer diameter, 60 mm inner diameter, and 1.5 mm thick, immersed in a cylindrical tank of water with a diameter of 500 mm by 180 mm high, with the annular disk 80 mm below the free surface of the water. The disk is placed on a compliant suspension such that the first disk mode is enough above the suspension mode to simulate a free-free boundary condition. The test is used to generate the NAVMI factors; Figure 6 (from Kwak) plots these for the plate resting on the surface of the liquid, where $\delta = \frac{b}{a}$ (ratio of inner radius to outer radius), s is the number of nodal diameters, and n is number of nodal circles. These values are multiplied by 2.0 for full immersion in the liquid. Similar charts are presented for (s, n)= (1,1), (2,1), and (s,n)=(2,0), (3,0).

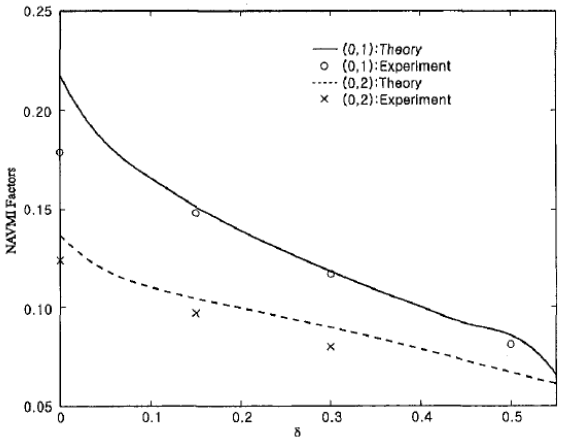

Figure 6. NAVMI factors versus δ; (s, n) = (0,1), (0,2)

A numerical analysis is now performed for the annular disk using the same process as that followed for the rectangular plate. The properties used for the disk are the same as used by Kwak. The results agree well with the theoretical values using Kwak's equation, as the relative error is less than 3% for both a semi-infinite theoretical boundary case and the experimental cases for all mode shapes. This agreement helps to validate the numerical analytical procedure.

A parametric study is then undertaken to see the effect of density on the modal characteristics of the annular disk. In addition to air and water, typical rocket engine fluid media such as LH2, kerosene, and LOX are used to get a wide range of fluid densities. The results of this study are shown in Figure 7, where the mode shapes are identified by their number of nodal diameters (ND) and nodal circles (NC), and the marks on the curves correspond to the density of the previously mentioned propellants, respectively.

The results show that the modal order is generally not mismatched (i.e., the curves do not intersect), although there are two exceptions, the 3 ND, 1 NC mode shape and the 0 ND, 2 NC mode shape. These results support the hypothesis that mode number switching is dependent on the symmetry of the structure and its boundary conditions, since this case is completely symmetric.

LOX PUMP INDUCER

As the inducer is a complicated geometry, no analytical solution for the modal characteristics in fluid exists. However, the numerical modeling procedures developed and verified using the simpler geometries can be applied, and the results compared with modal testing in both air and water. The basic material properties of the blade are a density of 8193 kg/m^3, Young's Modulus of 202.71 Gpa, and Poisson's Ratio of 0.29. The fluid domain is defined to match the cylindrical enclosure used for the immersed modal test (Figure 8), which has a 19.53 cm diameter and 24.769 cm height. The structural mesh was generated using a CAD model with a number of detailed features inside the hub (not in contact with the fluid) removed to reduce the model size, a high mesh density used for the inducer blades, and the base of the inducer hub fixed (see Figure 9). The fluid/structure interface surfaces were specified at all inducer/hub locations except for the fixed hub surface.

As a first step, a modal analysis in vacuum is now performed and the results compared with the modal test in air. For the first 18 modes up to 2900 Hz, the error is less than 2% and only two of the frequencies have an error of more than 5%, suggesting that the model is accurate. Next, a modal analysis in water is performed and compared with the analogous modal test. Numerous problems had to be overcome to achieve reproducible results in this submerged modal test, including air

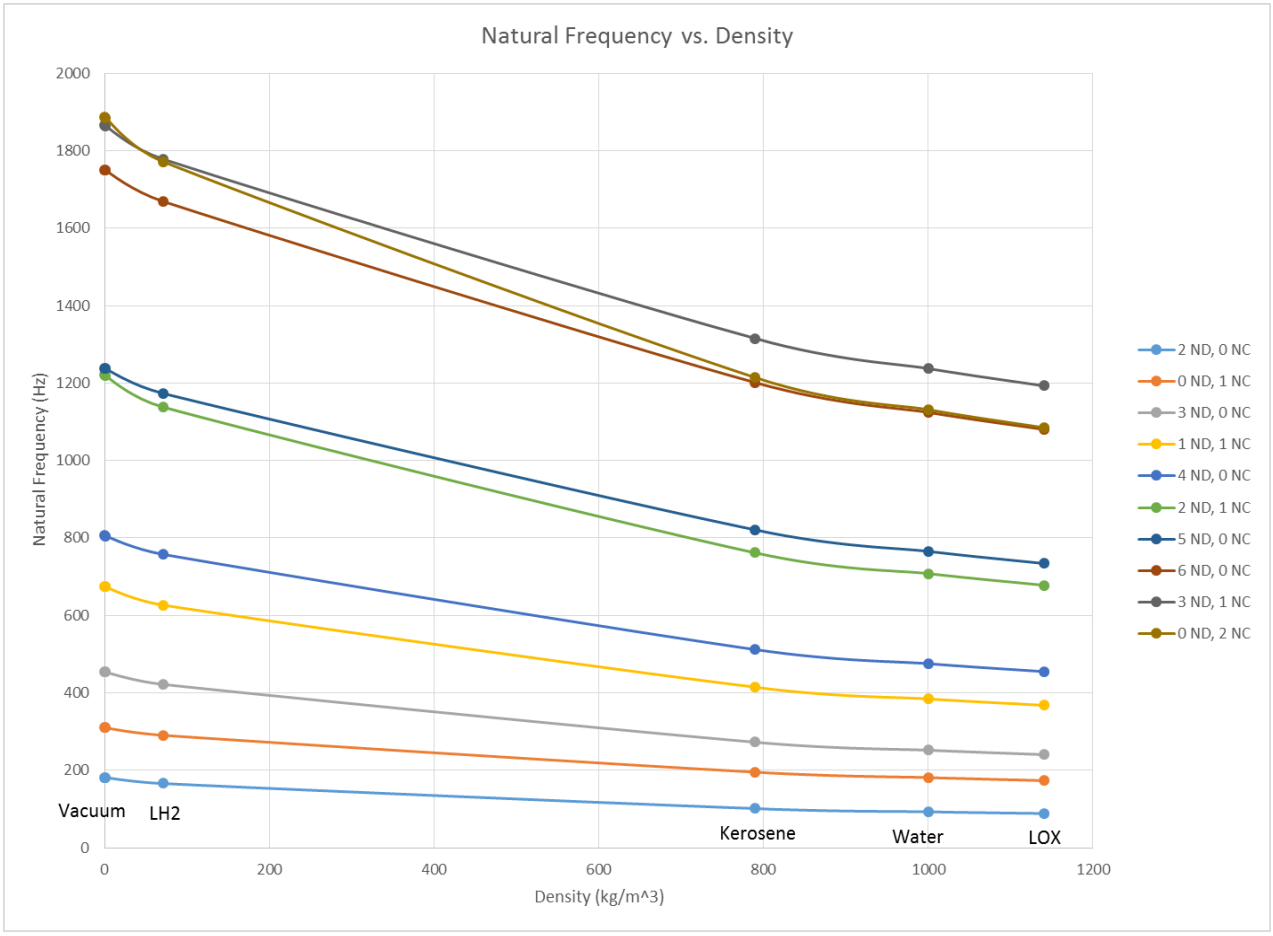

Figure 7. Annular Disk Natural Frequency vs. Immersed Fluid Density

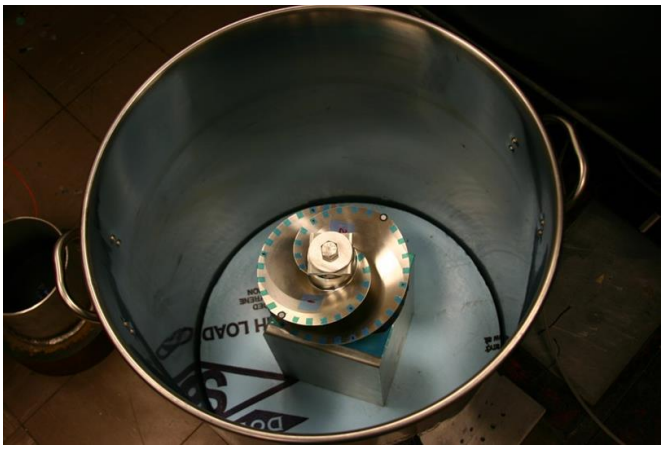

Figure 8. Setup of immersed modal test

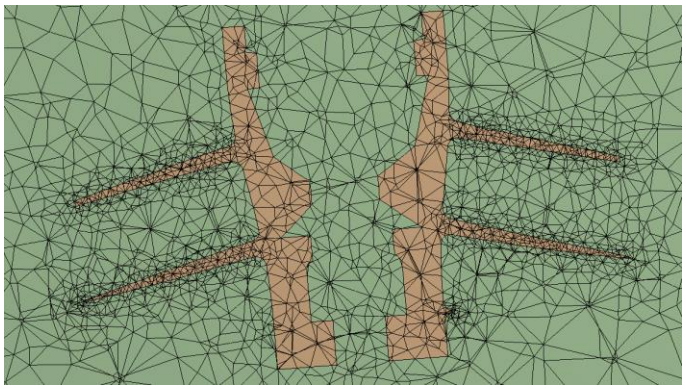

Figure 9. Cross-section of inducer solid mesh and surrounding fluid domain

bubbles and accessibility of the laser measurement system to the blades. These will tend to increase the error. Because of the limited access issue, only the frequencies from the test were obtained, and these are compared with the analytical frequencies in in Table 4. These results show excellent agreement, with the first 7 modes having an error of less than

2% and no errors above 10%. Mode 11 is omitted as it was not able to be identified in the modal test.

A parametric study is then performed to see the effect of density on the inducer blades, and the procedure is the same as the parametric study for the annular disk, except an additional fluid, methane, is added, which has a density of 421 kg/m^3 and sound speed of 1420 m/s. The runtime on a standard desktop Windows workstation was 20-30 minutes for each fluid.

Table 4. Comparison of FEA and Modal Test Natural Frequencies in Water

	Natural Frequency (Hz)		
Mode	Water (FEA)	Modal Test	Relative Error (%)
1	1020.4	1005.032	1.529106
2	1040	1036.007	0.385422
3	1075.2	1057.811	1.643866
4	1095.2	1090.148	0.463423
5	1152.4	1144.761	0.667301
6	1168.7	1189.042	1.710789
7	1187.6	1206.456	1.562925
8	1237.6	1287.035	3.840999
9	1253.2	1375.243	8.874286
10	1294.6	1414.22	8.458373
12	1431.9	1542.136	7.148267
13	1564.9	1593.773	1.811613

As with the studies using the simpler geometries, a method for qualitatively characterizing the modes is critical to enable successful tracing of the modes through different analyses for different densities. However, characterizing the mode shapes for the inducer is more difficult, as the mode shapes do not have clear, distinct shapes like the annular disk. Three elements of a mode shape are used for this characterization; a numerical value representing the amount of wavelengths along one blade, assessment of whether the shape is either sinusoidal, parabolic, or a combination of both, and whether the shape is in-phase (IP) or out-of-phase (OP), which refers to one blade with respect to the other. Examples of these different descriptive parameters are shown in Figures 10 through 13. Figure 11 can be used to explain the difference between sinusoidal and parabolic motion. It can be seen that in both shapes, the middle of the blade has either zero or very little displacement. However, in sinusoidal motion, the sides of the blades move 180 degrees out-of-phase with each other, as seen in the top picture, while in parabolic motion, both sides of the blade move up or down in-phase, which is seen in the bottom picture.

In addition, there are some mode shapes that could not be described using the same method detailed above, as there is some hub movement in the mode shape and the number of wavelengths associated with the hub movement is not consistent throughout the fluids. The hub may move from one direction to another or it may twist as well. All of the descriptions are used to create a plot (Figure 14) that traces the natural frequency variation with respect to density; mode shapes with hub movement or parabolic motion are not seen in all the density cases and so are omitted from the graph.

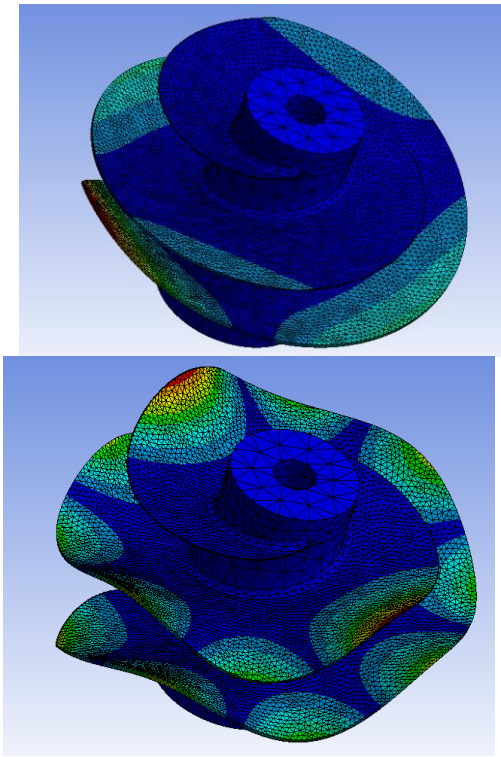

Figure 10. Example of 1.5 Wavelength Mode Shape (top), 4 wavelength shape (bottom)

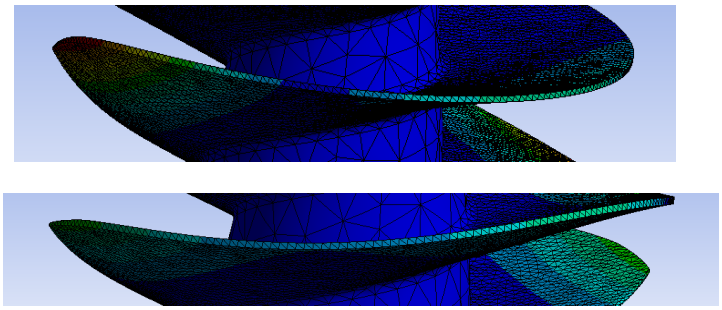

Figure 11. Sinusoidal motion (top), parabolic (bottom)

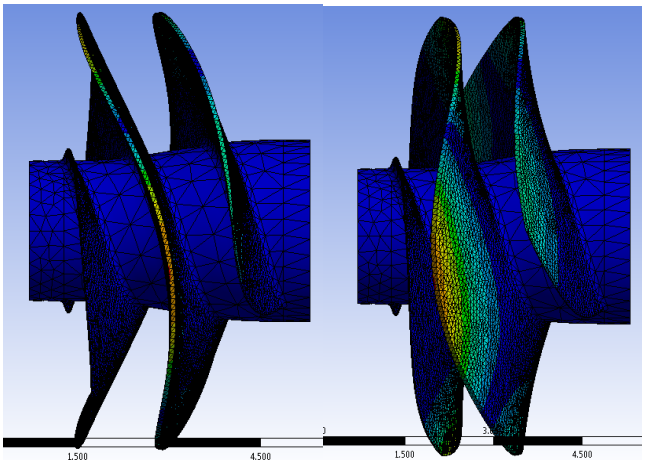

Figure 12. Example of Blades Moving In-Phase

By comparing Figure 14 to Figure 7, it is clear that there are more frequency crossings between mode shapes for the inducer blades compared to the annular disk. The crossings appear to occur only when an IP mode switches with an OP mode, which have very close frequencies. The modal number mismatching also appears to occur generally at the lower values of density. Table 5 shows a qualitative comparison of the first 20 modes. These show that the shapes themselves do not vary significantly, but that the relative numerical order of their associated natural frequencies do change with density. These changes in order and/or shape are highlighted. A notable

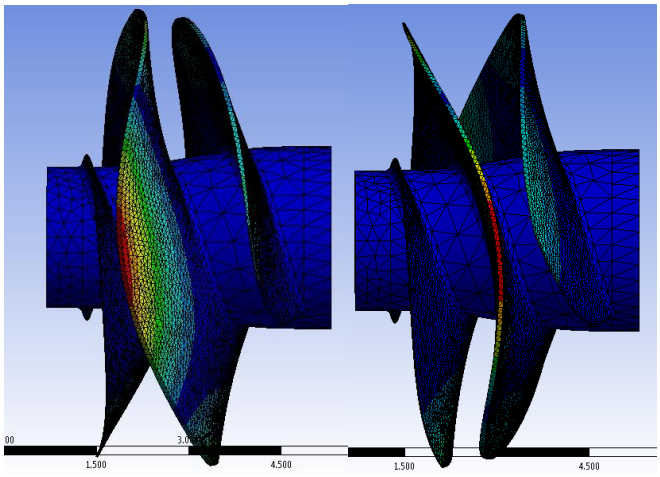

Figure 13. Example of Blades Moving Out of Phase

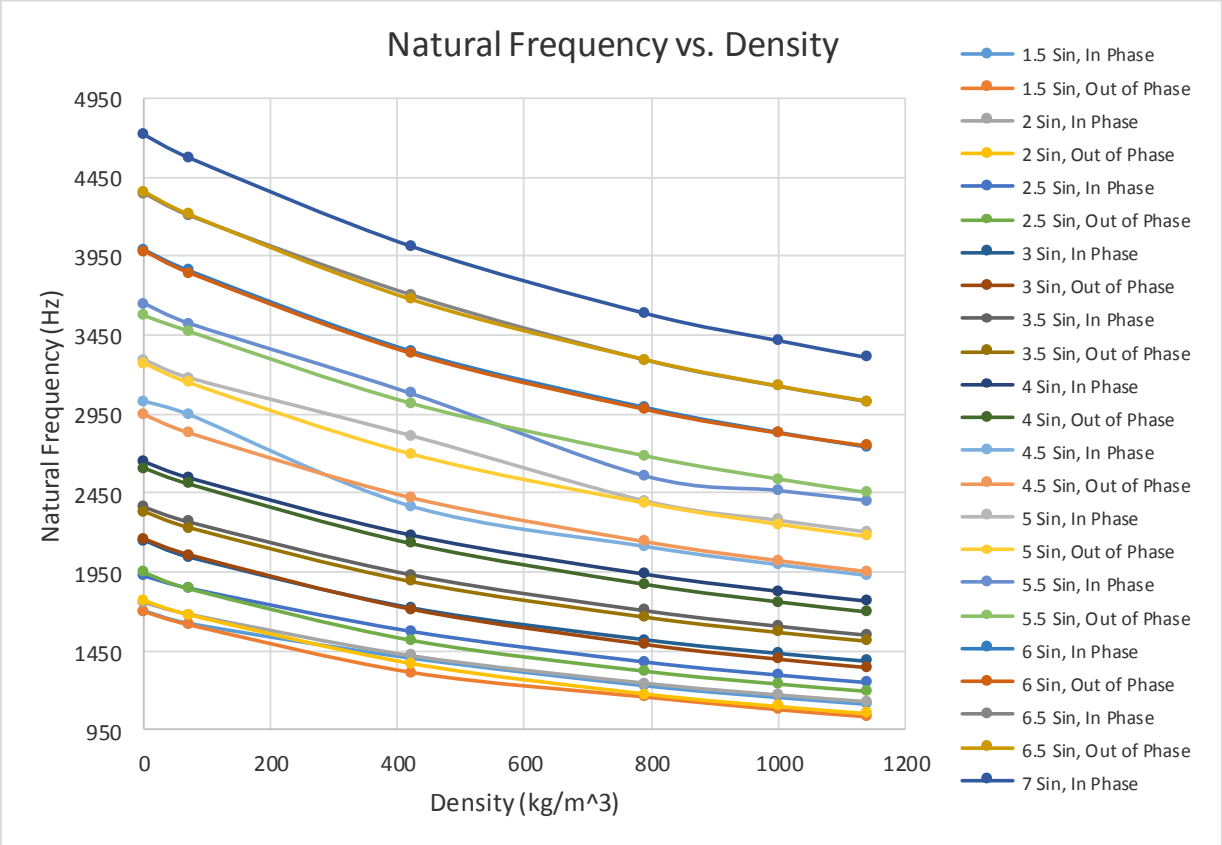

Figure 14. Natural Frequency vs. Density for Different Mode Shapes

observation is that for most of the mode shape pairs, the out-of-phase mode shape is usually the one with lower frequency when the blades are immersed in a fluid as compared with vacuum, where the in-phase mode usually has the lower frequency (an exceptions is the 4.5 and 5.5 wavelength pairs).

MAC analysis was also performed on the LH2-Vacuum combination and the LOX-Vacuum combination, and verify the qualitative assessments. The values for the first comparison are all close to 1.0 along the diagonal with the exception of mode-swapping between modes 4 and 6 and modes 7 and 8, which are on the corresponding off-diagonal location. In contrast, the LOX-Vacuum MAC has only a single high value, showing the significant change in the mode shapes (see Table 6), although there are some other values above 0.7 within the first 30 modes, indicating a partial shape change.

As much of the change in mode number mismatching occurs in the lower density range, several supplemental cases in the mid-density region that are not for realistic propellants are added to the analysis. These cases are at ρ = 150, 275, and 300 kg/m^3. Examination of the mode shapes, which shows total deformation, (Figure 15) shows that the one-wavelength sine occurs between 150 and 200 kg/m^3, with the half-wave in the 1.5 sine at lower densities gradually disappearing. In the top picture, it can be seen that the blue area on the blade shifts upward when comparing to the bottom picture. The blue area signifies no movement on the blade, so as it reaches the top of the blade, the mode shape of the blade is 1 sine wave and not 1.5 sine waves anymore. This mode also eventually becomes mode number 1. Another observed trend is that as the density increases, the number of parabolic and sine wave modes decrease, from four for vacuum, three for ρ=150, and to two for ρ=275 and higher. Finally, hub bending and twisting start, which do not move much fluid, becoming noticeable for higher modes, thereby playing a role in the mode number switching and lessening the frequency reduction for these modes.

Another valuable result from this study is obtaining a more thorough quantification of the "knockdown" factor mentioned in the introduction. This factor as a function of density is plotted is plotted in Figure 16. In general, these factors decrease going from the lower frequency mode shapes to the higher frequency mode shapes, e.g., the lowest knockdown rate for almost all of the fluids is the 7 sine, IP mode shape, which occurs at the highest frequency out of all of the mode shapes calculated. On the other hand, the 2 sine, OP mode shape has the highest knockdown factor for the higher density fluids. Table 7 shows the range of factors and the average values per propellant case; it is also apparent from this table that the range of factors increases with the density. These ranges are all less than the 20% range (20-40% knockdown) estimate used before this study.

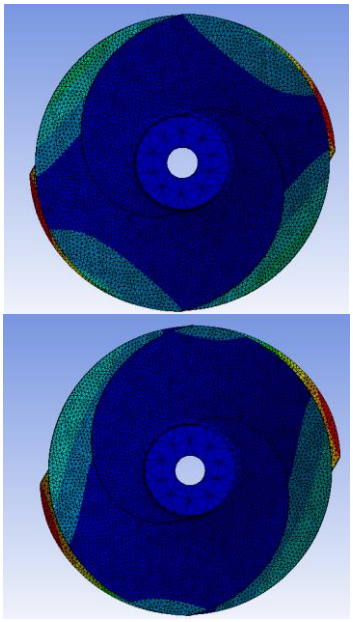

Figure 15. MN 2, top LH2, bottom ρ=200 kg/m^3

CONCLUSIONS AND FUTURE WORK

A number of valuable conclusions can be drawn from this study. First, knockdown factors for a specific fluid are not constant but instead are dependent on the mode shape, although the largest this variability gets is about 10% for LOX, the densest fluid. The factors decrease the most for lower frequency shapes and less for higher ones. It follows, therefore, that mode number mismatch between air and fluid operation becomes not only possible, but common, as a knockdown factor for a particular mode shape may be higher than for another mode shape. Since this is a function of added mass, the mismatch is more prevalent for higher density fluids, but it initiates even for very low density ones.

Another important conclusion reached is that it appears that the basic mode shapes of a structure do not change if it is fully symmetric, which includes its geometry and boundary conditions. There is some indication of small changes in the relative magnitudes within the mode shape. This conclusion is evident in the results from the cantilever rectangular plate and the inducer, which are not symmetric, and the fixed-fixed plate and the annular disk, which are. For non-symmetric structures, though, the mode shapes almost universally change for dense fluids, as shown by the very low MAC calculations. For the inducer in particular, the changes follow a trend of reduced parabolic and sine wavelengths with increasing density.

Table 5. Modal Trace with Density Variation

#	Vacuum	LH2	Methane	Kerosene	LOX
1	1.5 sin w/lengths, OP	1.5 sin, OP	1 sin, OP	1 sin, OP	1 sin, OP
2	1.5 sin w/lengths, IP	1.5 sin, IP	1.5 sin, OP	1.5 sin, OP	1.5 sin, OP
3	1 Parabolic, 1 Sin, IP	1 Parabolic, 1 Sin, IP	1.5 sin, OP	1.5 sin, OP	1.5 sin, OP
4	2 sin, IP	1 Parabolic, 1 Sin, OP	2 sin, OP	2 sin, OP	2 sin, OP
5	2 sin, OP	2 sin, OP	1.5 sin, IP	1.5 sin, IP	1.5 sin, IP
6	1 Parabolic, 1 Sin, OP	2 sin, IP	2 sin, IP	2 sin, IP	2 sin, IP
7	2.5 sin, IP	2.5 sin, OP	Parabolic, Sin, OP	Parabolic , Sin, OP	Parabolic, Sin, OP
8	2.5 sin, OP	2.5 sin, IP	2.5 sin, OP	2.5 sin, OP	2.5 sin, OP
9	1.5 Parabolic, 1 Sin, OP	1.5 Parabolic, 1 Sin, OP	Parabolic, Sin, IP	Parabolic, Sin, IP	Parabolic, Sin, IP
10	1.5 Parabolic, 1 Sin, IP	1.5 Parabolic, 1 Sin, IP	2.5 sin, IP	2.5 sin, IP	2.5 sin, IP
11	3 sin, IP	3 sin, IP	3 sin, OP	3 sin, OP	3 sin, OP
12	3 sin, OP	3 sin, OP	3 sin, IP	3 sin, IP	3 sin, IP
13	3.5 sin, OP	3.5 sin, OP	3.5 sin, OP	3.5 sin, OP	3.5 sin, OP
14	3.5 sin, IP	3.5 sin, IP	3.5 sin, IP	3.5 sin, IP	3.5 sin, IP
15	4 sin, OP	4 sin, OP	4 sin, OP	4 sin, OP	4 sin, OP
16	4 sin, IP	4 sin, IP	4 sin, IP	4 sin, IP	4 sin, IP
17	4.5 sin, OP, hub bend	4.5 sin, OP, Hub Bend	4.5 sin, IP	4.5 sin, IP	4.5 sin, IP
18	4.5 sin, IP, Hub Bend	4.5 sin, IP, Hub Bend	4.5 sin, OP	4.5 sin, OP	4.5 sin, OP
19	4.5 sin, OP	4.5 sin, OP	5 sin, IP, W to E	5 sin, OP	5 sin, OP
20	4.5 sin, IP	4.5 sin,IP	5 sin, OP	5 sin, IP	5 sin, IP

Table 6. MAC between LOX and Vacuum

LOX	Vac/1	2	3	4	5	6	7	8	9
1	0.00	0.14	0.00	0.01	0.00	0.71	0.00	0.13	0.00
2	0.66	0.00	0.19	0.00	0.02	0.00	0.00	0.00	0.07
3	0.00	0.47	0.00	0.30	0.00	0.00	0.00	0.10	0.00
4	0.00	0.00	0.05	0.00	0.90	0.00	0.01	0.00	0.00
5	0.26	0.00	0.68	0.00	0.05	0.00	0.01	0.00	0.00
6	0.00	0.45	0.00	0.38	0.00	0.13	0.00	0.00	0.00
7	0.14	0.00	0.10	0.00	0.01	0.00	0.12	0.00	0.34
8	0.00	0.03	0.00	0.28	0.00	0.16	0.00	0.43	0.00
9	0.00	0.00	0.00	0.09	0.00	0.04	0.00	0.16	0.00

Table 7. Knockdown Factor Ranges and Averages

Fluid	Factor Range	Average Factor
LH2	2.8 – 5.3%	3.9%
Methane	14.8 – 22.6%	18.1%
Kerosene	24.0 – 33.5%	28.0%
Water	27.6 – 38.0%	32.0%
LOX	29.9% – 40.5%	34.4%

It is critical to recognize the change in mode shape for several reasons. First, model updating with modal test becomes problematic if the shapes change. Second, design to avoid resonance is highly critical on the mode shape for modes other than the primary ones, as resonance is only a factor when the excitation shape matches the mode shape. Finally, application of the modal superposition method of forced response analysis is dependent on the use of accurate mode shapes.

A more-refined assessment of the "knockdown" factor values and ranges than any previously reported in the literature for a realistic engineering structure is also presented in this paper. This data is of tremendous benefit for preliminary analysis and design, where a quick estimate is necessary. These results are important not just for rocket engine turbomachinery, but for water pumps and turbines, propellers, and any other structure operating in a heavy fluid with dynamic excitation.

The clear avenue for future work for this endeavor is to expand the analytical techniques discussed in the literature to develop analytical expressions and justification for the mode shape changes and associated frequency knockdowns. These expressions must be able to accurately predict the functional relationship to the shapes, which will enable accurate tracing of the mode number from vacuum analysis (or testing in air) to analysis and operation in the intended fluid environment.

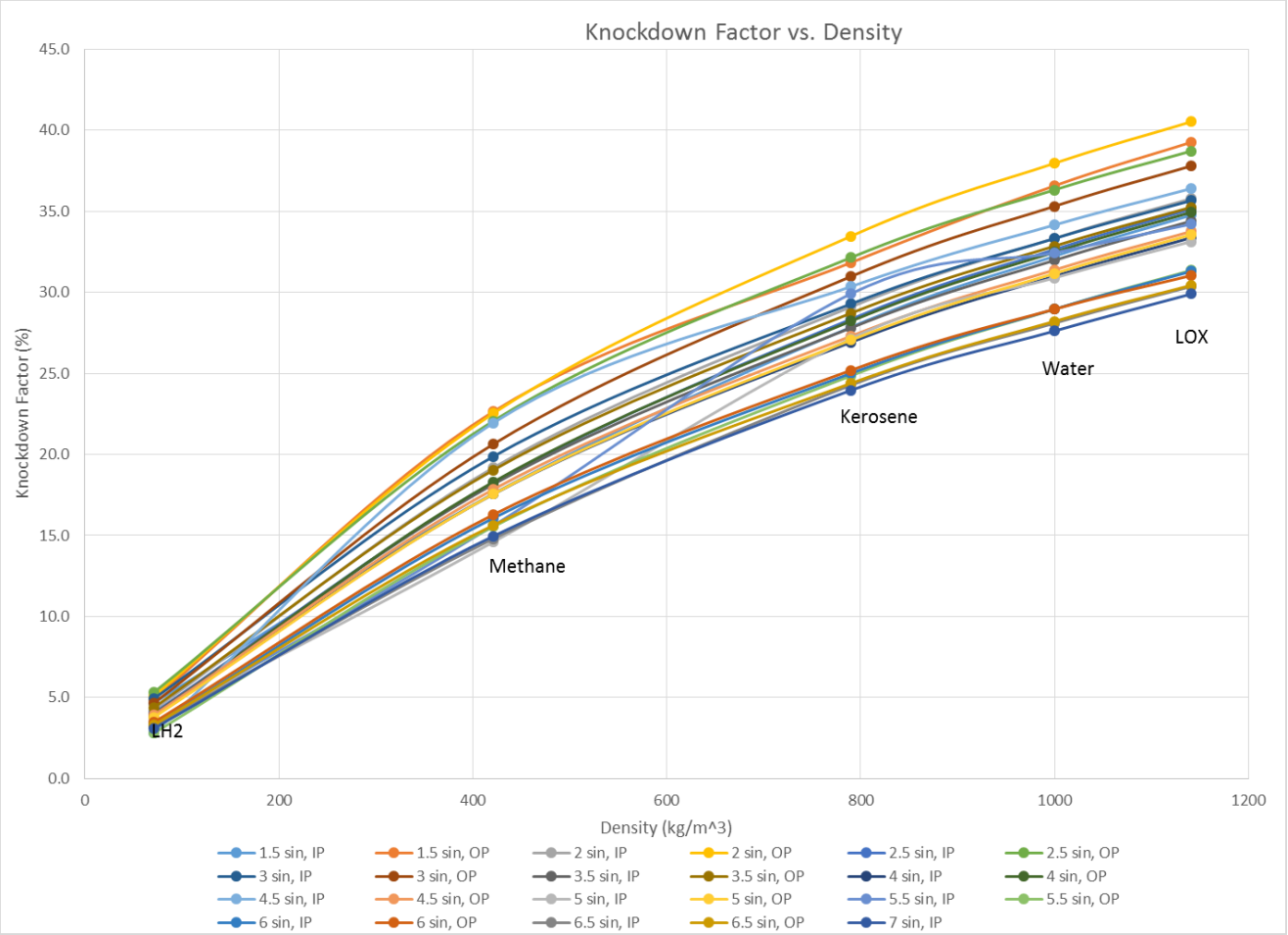

Figure 16. Knockdown Factor vs. Density

ACKNOWLEDGMENTS

The first author would like to thank Dr. Andrew Brown for serving as his mentor and for help in understanding essential concepts in structural dynamics during the 2016 NASA student summer internship program, when the bulk of this research was performed. He also would like to thank Jennifer DeLessio of MSFC/Jacobs for substantial assistance in the use of the structural and acoustic modeling capabilities in the ANSYS software code.

REFERENCES

[1] Lindholm, U, et. al., "Elastic Vibration Characteristics of Cantilever Plates in Water," Journal of Ship Research, June 1965, pp. 11-36.

[2] Kwak, M. K, "Hydroelastic Vibration of Free-Edge Annular Plates" J. Vib. Acoust. Journal of Vibration and Acoustics 121.1 (1999)

[3] Askari, E., Jeong, K-H., Amabili, M., "Hydroelastic vibration of circular plates immersed in a liquid-filled container with free surface," Journal of Sound and Vibration 332 (2013) 3064-3085.

[4] Kerboua, Y., Lakis, A.A., Thomas, M., Marcouiller, L., Vibration analysis of rectangular paltes coupled with fluid," Applied Mathematical Modelling 32 (2008) pp. 2570-2586.

[5] Hosseini-Hashemi, S., Karimi, M. , Rokni, H., Natural frequencies of rectangular Mindlin plates coupled with stationary fluid," Applied Mathematical Modelling 36 (2012) pp. 764-778.

[6] Blevins, Robert D., Formulas for Natural Frequency and Mode Shape, Krieger Publishing Company, Florida, 1979, pp. 236-290.

[7] ANSYS, Inc. Lecture Notes, "AACTx_R170_L-02_Modal Analyses.pdf," 2016.

[8] Davis, R.B, Virgin, L.M., Brown, A.M., "Cylindrical Shell Submerged in Bounded Acoustic Media: A Modal Approach," AIAA Journal, Vol. 46, No. 3, (752-763)